Hindawi
Advances in Meteorology
Volume 2018, Article ID 7293987, 15 pages
https://doi.org/10.1155/2018/7293987

Research Article

Assessment of Ground-Based and Aerial Cloud Seeding Using Trace Chemistry

James M. Fisher[1,2] **Marion L. Lytle**[1] **Melvin L. Kunkel**[2] **Derek R. Blestrud**[2] **Nicholas W. Dawson**[2] **Shaun K. Parkinson**[2] **Ross Edwards**[3,4] **and Shawn G. Benner**[1]

[1]*Department of Geosciences, Boise State University, Boise, ID 83725, USA*
[2]*Idaho Power Company, Boise, ID 83702, USA*
[3]*Physics and Astronomy, Curtin University, Perth, WA 6845, Australia*
[4]*Department of Civil and Environmental Engineering, UW-Madison, Madison, WI 53706, USA*

Correspondence should be addressed to Shawn G. Benner; sgbenner@gmail.com

Received 31 August 2017; Revised 12 December 2017; Accepted 25 December 2017; Published 19 February 2018

Academic Editor: Steven Siems

Targeting seedable clouds with silver iodide in complex terrain adds considerable uncertainty in weather modification studies. This study explores the geographic and temporal distribution of silver iodide associated with an active cloud seeding program in central Idaho snowpack using trace chemistry. Over 4,000 snow samples were analyzed for the presence of a cloud seeding silver iodide (AgI) signature over two winter seasons. The results indicate the following. (1) At sites within 70 km of AgI sources, silver enrichments were detected at 88% of cases involving seeding efforts from ground generators, but none from aircraft seeded cases. (2) Real-time snow collection methods were replicable within 0.41 ppt and confirmed seeding signatures for the entire duration of a seeded storm ($n = 3$). (3) Sites sampled beyond 70 km of AgI sources ($n = 13$) lacked detectable seeding signatures in snow. The results of this study demonstrate some of the strengths and limitations of chemical tracers to evaluate cloud seeding operations and provide observational data that can inform numerical simulations of these processes. The results also indicate that this chemical approach can be used to help constrain the spatiotemporal distribution of silver from cloud seeding efforts.

1. Introduction

The National Research Council stated that targeting seedable clouds with silver iodide (AgI) in complex terrain is a high priority research item for the weather modification community [1]. The Bureau of Reclamation's literature review of cloud seeding studies mirrors this opinion stating *"[determining when and where AgI nucleates snow] has been described by many weather modification researchers as the single most critical issue that has compromised the success of both operational as well as research field projects"* [2].

One method of inferring approximately when an AgI plume passes over location(s) is by measuring Ag concentrations in snow. High silver concentrations in snow (irrespective of passive tracers) is a strong indicator of when and where seeded snow is deposited [3, 4]. Although trace chemistry does not provide evidence on the relative change in precipitation, it does provide boundaries on when AgI could have impacted precipitation [5]. Conversely, trace chemistry can also highlight when an AgI plume passes over a control site [6, 7] and potentially impact statistics in randomized seeding schemes.

Determining the spatial and temporal distribution of AgI in snow has been especially useful in the past 5 years for validating and developing cloud seeding process models [8, 9]. Two recent cloud seeding projects utilized snow chemistry data to inform statistical models or to parameterize weather model inputs: SNOWIE and the WWMPP [10–12]. Models are rapidly advancing the ability to predict when and where AgI are active [10], but considerable uncertainties remain in these models regarding how nucleation and subsequent transport and deposition are parameterized [12].

Although the usefulness of trace chemical methods is recognized by the cloud seeding community [13], considerable knowledge gaps remain. Some trace chemical studies report that roughly 80% of samples within the anticipated area of precipitation enhancement ("target zone") did *not* contain silver concentrations reflective of cloud seeding signatures [5, 14]. However, no peer-reviewed research has compared the detectability of Ag signatures sourced from aircraft and ground generators. Secondly, the utility of real-time sampling during deposition has not been rigorously evaluated. Although several studies have used real-time sampling techniques [5, 14, 15], more work is needed to show the replicability of Ag enrichments in terms of both concentration and the capacity to temporally constrain the timing of AgI deposition. Third, the detectability of AgI in snow downwind of the target area has not been explored since 1971 [16]. Advances in lab technology and ultraclean environmental sampling warrant further investigation of downwind Ag enrichments.

The three objectives of this study are to (1) evaluate the spatial and temporal distribution of cloud seeding signatures associated with both ground- and aircraft-generated cloud seeding; (2) develop a real-time sampling approach to determine the replicability of the concentration and timing of Ag enriched snow, and (3) evaluate the downwind extent of seeding signatures in snow. Using the source-receptor approach, this study analyzed more than 4,000 snow samples over the course of two winter seasons. Sample collection takes place in the area targeted for precipitation enhancement and up to 180 km downwind. These observations provide a validation dataset for cloud seeding process models and spatially and temporally constrain when AgI may have impacted precipitation.

2. Data

2.1. Study Area. Since 2003, Idaho Power Company (IPC) has been operationally cloud seeding the Payette River Basin, 50 km NE of Boise, Idaho (Figure 1). The additional snow from this program feeds into the Snake River, where a series of hydroelectric dams generate roughly half the energy produced by IPC. The Payette River Basin ranges in elevation from 650 m to 3,110 m and receives between 300 mm and 1,700 mm annually, which primarily falls as snow from November to April.

IPC cloud seeding operations utilize both ground generators and aircraft. Each of the 17 remotely controlled ground generators in the Payette River Basin releases 20 g h^{-1} of AgI during operation. Two aircraft dedicated to IPC's cloud seeding program release AgI using burn-in-place flares (releases 16.2 g of AgI in 3.5 minutes) and aircraft ejectable flares (releases 2.2 g of AgI over 35 seconds). Decisions on the operation of generators and aircraft are based on weather forecasts by trained meteorologists.

2.2. Spatial Snow Samples. To evaluate the spatial distribution of Ag, field teams collect snow samples from freshly fallen snow deposited during a seeded precipitation event. Spatial samples are collected in a series of snow pits (hereafter, the "snow pit method") across the enhancement target area. This method entails excavating and inserting 3 cm diameter (50 mL) polypropylene vials (Fisherbrand, Pittsburgh, PA, USA) orthogonal to the snow pit face. This method also requires the collection of two profiles at each snow pit for replication purposes.

Timing and location are key to achieving replicable trace chemical data. Minimizing the time between the seeded storm and sample collection reduces photolytic effects on silver concentrations in snow [17], wind redistribution [18], snow compaction, and migration of trace elements through the snowpack [19]. Therefore, field teams collect samples within 48 hours of a seeded storm from remote, flat clearings that are effectively shielded from wind and are in a shaded area. Technicians strictly adhered to clean field techniques [20] throughout to reduce the potential for anthropogenic contamination.

2.3. Temporal Snow Samples. The "real-time sampling method" constrains the timing of seeding signatures in snow. In this method, samples are collected at a location over time during the seeded precipitation event. Three triple-cleaned 669 mL polypropylene containers (Rubbermaid, Hoboken, NJ, USA) remain open until about 10 grams of snow is collected (visually estimated). Setting a minimum mass as the threshold maximizes the temporal resolution of resulting observations. Real-time sample collection frequency typically ranges from 15 and 45 minutes, depending on precipitation intensity.

To reduce contamination potential during real-time sampling, technicians divide tasks based on equipment cleanliness. While one technician collects samples and only handles triple acid-washed equipment ("clean hands"), another technician measures relevant snow properties with less clean equipment ("dirty hands") [21]. "Dirty hands" measures snow depth, snow temperature, and SWE at each time step 100 m downwind of the polypropylene containers. One drawback of this method is 100 m is beyond the correlation length of snow [22]. Therefore, precipitation amounts and density measurements by "dirty hands" are likely not identical to snow samples in the polypropylene containers upwind. However, this is an effective method to mitigate contamination. Currently, the project average Ag standard deviation between field replicates is 0.41 ppt ($n = 86$ samples in 28-time intervals).

2.4. SNOTEL. The National Resource Conservation Service (NRCS) owns and operates fully automated SNOw TELemetry (SNOTEL) stations. SNOTEL stations provide a nearly continuous record of hourly snowpack conditions such as snow depth (using ultrasonic snow depth sensors) and snow water equivalent (using snow pillows). Although the NRCS performs quality control checks, there are known uncertainties with published snow water equivalent. For instance, ice bridging, snow creep, deposition of foreign material, and changes in surrounding landscape alter snow accumulation measurements [23–25]. These mechanisms can cause precipitation errors as high as 30% [22]. However,

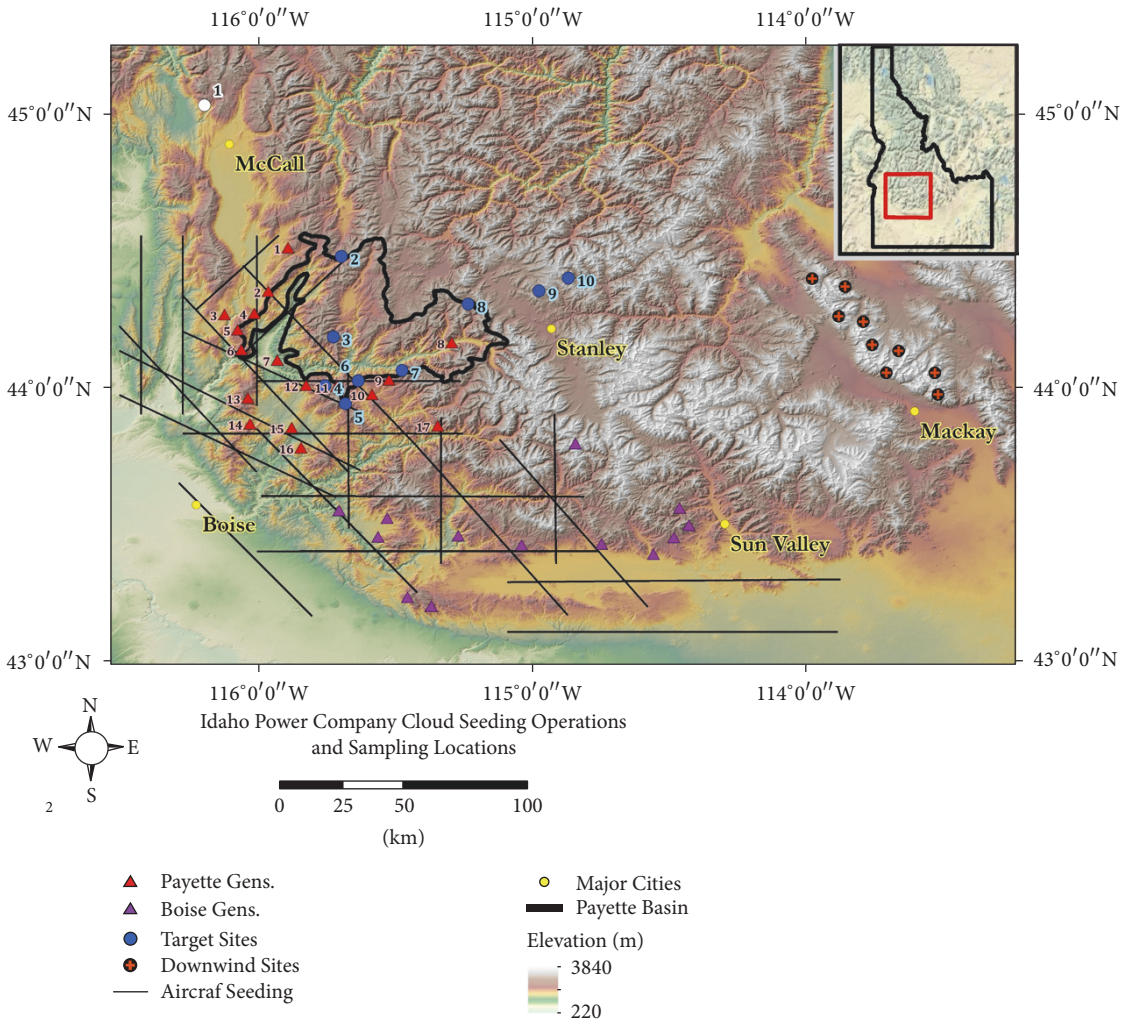

FIGURE 1: IPC uses ground generators (red triangles) and aircraft (lines) to deliver AgI. Sampling sites in and around the Payette River Basin were targeted for precipitation enhancement (blue dots). Sites downwind of operations were sampled as well (orange crosses). Site 1 (white dot) was the sole control site for this project.

the snow water equivalent measurements were adequate to estimate when spatial samples were deposited.

3. Methods

The overall experimental method follows the source-receptor approach, where Ag concentrations serve as a proxy for when and where AgI plumes directly affect ice nucleation [6, 7, 26], for linking microphysical changes of snow to AgI [13, 26, 27], and for model validation [12]. This approach has historically proven to be challenging due to low Ag signal-to-noise ratios in snow and the need for ultratrace laboratory equipment and protocol [28, 29]. However, beginning in the 1990s, instrumental detection levels for metals improved dramatically. With the improved detection limits came the realization that much of the data before 1990 was contaminated during sample collection and analysis. The importance of ultraclean protocol in the field and laboratory was recognized and is now widely implemented [30, 31]. Today, the refined methods of the source-receptor approach make it reliable and economically feasible for operational use.

3.1. Laboratory Analysis. Samples are acidified as per the EPA Direct Analysis Method 200.8 [32]. This acidification method is ideal primarily because it is the conventional method for analyzing precipitation and natural waters. Samples are acidified to 2% HNO_3 (Seastar Chemicals, BASELINE®, Lot number 1214070) and stored at room temperature to thaw. Once acidified, samples are stored in the dark for 24 hours within the Class 100 clean room prior to analysis. Adopting this method allows for direct comparison with other studies, because ultratrace element concentrations are influenced by both acidification strength [33] and storage time at room temperature [34].

Samples are prepared in the clean lab prior to transport to the Thermo Scientific X-Series 2 Inductively Coupled-Plasma Mass Spectrometer (ICP-MS) laboratory (not a Class 100 clean room). After the 24-hour acidification period,

Table 1: Operating ICP-MS conditions and acquisition parameters.

Parameter	Setting value
Forward power	1400 W
Cooling	13 L/min
Expansion pressure	$2.0 * 10^{0}$ mbar
Analyzer pressure	$4.0–4.2 * 10^{-7}$ mbar
Turbo pump speed	1000 Hz
Vacuum pump load	0.8–1.2 A
Pole bias	1.0
Hex bias	4.0
Sample cone	Ni, 1.1 mm aperture inner diameter
Microskimmer cone	Ni, 0.8 mm aperture inner diameter
Sample depth	Adjusted daily[1]
Lens settings	Adjusted when appropriate
Nebulizer back pressure	~2.0 bar, optimized daily[1]
Nebulizer Flow Rate	400 μL/min
Sample Uptake Time	20 s
Rinse Time between samples	20 s
Elements measured	Na, Al, Cr, Co, Sr, Ag, Ba, La, Ce, Pb
Dwell time per element	Ag: 200 ms; Na, Al, Cr, Co, Sr, Ba, La, Ce, Pb: 10 ms

[1]Optimized to obtain a stable/high 115 In signal (>500,000 cps for 10 ppb) min. oxide formation rate.

Table 2: Mean crustal concentration (X_{crust}) to compute CEF *(equation (1))*.

Element	Ag	Al	Ce	Sr	Ba
X_{crust} [g g^{-1}]	50×10^{-9}	80×10^{-3}	64×10^{-6}	350×10^{-6}	550×10^{-6}

samples are decanted from the 50 mL polypropylene field vials to the 15 mL Teflon vials in the clean lab (Savillex, Eden Prairie, MN, USA). Test vials are sealed with Parafilm, placed in a clean polyethylene rack, and sealed again in a clean polyethylene tub before transport to the ICP-MS laboratory. The polyethylene sample rack is loaded directly into the Elemental Scientific Inc. SC-FAST Automated Sample Introduction System, housed in an AirClean AC4000 Workstation. The AirClean Workstation substitutes for a clean room environment during sample analysis.

The ICP-MS is calibrated using three serial dilutions of 1,000 mg/L (1,000 ppm) standards to analyze the following crustal tracers: Na, Al, Cr, Co, Sr, Ba, La, Ce, and Pb. Ag is calibrated using serial dilutions of 1,000 ppm to concentrations to 100 parts per trillion (ppt), 50 ppt, 10 ppt, and 1 ppt. The Ag calibration linear regression lines are recalibrated a minimum of 3 times per analysis to minimize drift. Drift is further mitigated by analyzing a 10 ppb indium internal standard throughout the analysis. Blank (2% HNO_3) rinses followed each calibration to reduce memory effects from 50 ppt and 100 ppt standards. Blanks are also analyzed every 10 samples to ensure instrument precision. A list of other ICP-MS standard operating conditions is in Table 1.

3.2. Distinguishing Seeding Signature from Background Silver Concentrations. In the source-receptor approach, it is essential to distinguish the source of high Ag concentrations. High Ag concentrations in snow can occur from terrestrial dust, from anthropogenic contamination, or from Ag concentrations associated with cloud seeding. Terrestrial Ag can be found in snow at concentrations exceeding those expected from cloud seeding [5, 35]. A key tool to distinguish cloud seeded Ag from background Ag is the calculation of enrichment factor [36]. The enrichment factor accounts for sources of Ag contamination likely accompanied by elevated concentrations of other elements.

The crustal enrichment factor (CEF) filters out the most common source of naturally occurring silver in snow: aluminosilicate dust. The CEF is designed to highlight samples with high silver concentrations irrespective of elements commonly found in terrestrial dust using a normalizing approach (see (1)). Equation (1) normalizes these other elements by the mean concentration of the Earth's upper crust [37] as listed in Table 2. CEF values greater than two indicate silver concentrations are primarily sourced outside of aluminosilicate dust. CEF values close to one signifies all of the silver from a given sample is likely derived from dust.

Two criteria must be met for a sample to have a "seeding signature." First, a sample must have a Ag concentration at least 2 standard deviations above the mean naturally occurring Ag concentration [38]. Nonseeded snow in the Payette River Basin has silver concentrations of $\mu = 1$ ppt and $\sigma = 1$ ppt [38, 39]. Second, a sample must have a CEF greater than 2 to indicate significant Ag enrichments beyond the Ag

concentrations expected from snow rich in aluminosilicate dust:

$$\mathrm{CEF} = \mathrm{median}\left(\frac{\mathrm{Ag}_i/\mathrm{Ag}_{\mathrm{crust}}}{\mathrm{Al}_i/\mathrm{Al}_{\mathrm{crust}}}, \frac{\mathrm{Ag}_i/\mathrm{Ag}_{\mathrm{crust}}}{\mathrm{Ce}_i/\mathrm{Ce}_{\mathrm{crust}}}, \frac{\mathrm{Ag}_i/\mathrm{Ag}_{\mathrm{crust}}}{\mathrm{Sr}_i/\mathrm{Sr}_{\mathrm{crust}}}, \frac{\mathrm{Ag}_i/\mathrm{Ag}_{\mathrm{crust}}}{\mathrm{Ba}_i/\mathrm{Ba}_{\mathrm{crust}}}\right), \quad (1)$$

where CEF is crustal enrichment factor [unitless]; Ag_i is concentration of Ag in sample i [ppt]; X_i is concentration of element X in sample i [ppt]; X_{crust} is average concentration of element X in the Earth's crust [ppt].

3.3. Modeling Timing of AgI in Snowpack. A simple empirical model is used to convert snow depth to the time snow was deposited. Total precipitation in the field is obtained using a 200 cm^3 box density cutter. Density measurements are recorded at 3 cm intervals in the snow profile taken adjacent to column profiles in the snow pit.

$$p_i^* = \frac{P_s}{P_f} p_i, \quad (2)$$

where p_i^* is normalized hourly precipitation increments at the SNOTEL site [cm]; P_s is total precipitation from seeding event measurements at the SNOTEL station [cm]; P_f is total precipitation from seeding event measurements at the snow pit [cm]; p_i is SWE from 3 cm depth field density measurement [cm].

Equation (2) normalizes SWE measurements taken adjacent to chemistry samples for direct comparison with a nearby SNOTEL precipitation gauge (assuming the ratio of precipitation at the SNOTEL site and sampling site are constant). This approach creates an opportunity to relate SWE measurements in the snow pit to the timing of deposition metrics recorded by SNOTEL. The approximate timing of snow deposition is modeled using 1st-, 2nd-, and 3rd-degree polynomials (Figure 2(b)), chosen based on the most realistic trends and highest R^2 values. This method is most effective when snow is sampled within 48 hours of deposition.

3.4. Evaluating Downwind Extent. To evaluate the downwind distance in which Ag can be detected in snow, we performed two sampling campaigns (13 sites total) with at least one site >80 km downwind of AgI sources. The first campaign consisted of four sites with the Feb 18, 2016, ground generator storm event. These sites have samples collected at various distances from the nearest AgI source (up to 86 km away) and all parallel to the mean wind direction of at least one ground generator. The second transect consisted of nine sites roughly orthogonal to the mean wind direction and 180 km from the seeding source. These nine sites test whether seeding signatures are present and to test whether the seeding signature is continuous. Hobbs (1975) found seeding signature almost exclusively on the lee side of a targeted mountain range [40, 41]. To account for this local variability, three aspects of the Lost River Range were sampled: the windward slope, ridge, and the lee side of the range.

4. Results

4.1. Spatial Distribution of Cloud Seeding Signature. Over two winters, more than 4,000 snow samples were sampled and analyzed for silver enrichments reflective of a cloud seeding signature (http://scholarworks.boisestate.edu/geo_data/1/). These spatial sampling efforts represent a total of 35 snow pit locations (Figure 1) that extend over approximately 180 km and represent 14 seeded storm events (Table 4). Based on a >3 ppt Ag and an enrichment factor >2, 39% of samples collected in the target zone were identified as seeded. In all cases, replicates within snow pits were consistent; when one profile indicated a seeded snow sample, a signal was also observed in the replicate profile. The maximum observed Ag concentration in snow was 80 ppt. Ag enrichments in snow typically ranged from 5 to 25 ppt. Background concentrations of Ag in snow were 1.02 ppt measured at the control site (n = 178 samples, site 1 in Figure 1).

Spatial sampling data within the target zone show evidence that cloud seeding produces AgI snowpack signatures that are replicable across 10s of kms (Figure 3). For example, the Dec 4, 2015, storm that had a tap of Pacific moisture being advected into the target area from Northern California. This system produced a column of deep saturated air over the target area. The result of seeding this storm produced a double peak in Ag concentrations that was observed at 3 locations separated by approximately 30 km. Every seeded storm sampled at multiple sites showed similar basin-scale seeding signatures.

4.2. Comparing Ground and Aircraft Seeded Events. Surprisingly, there is a dramatic difference in occurrence of an AgI cloud seeding signature depending on the method of seeding (Table 3). To establish if seeding method impacted the presence of silver enrichments, seeding events were separated into three categories: ground generator only, aircraft only, and mixed (ground generator and aircraft seeding events). Ground generator only cases tend to be shallow, cooler systems with the bulk of the available moisture expected to be closer to the ground while aircraft-only cases tend to be warmer systems with the available moisture anticipated to be elevated within the cloud. In some instances, the region of moisture within the cloud can extend from near ground to at or above flight levels allowing for the use of both ground and airborne seeding. When these categories are separated, it is evident that nearly all ground-based seeding events are detected while aircraft Ag enrichments are rarely observed (discussion available in Section 5.2). Ag enrichments are found in 88% of the ground generator only event and none of the aircraft-only events (Table 3).

4.3. Temporally Constraining AgI. Real-time samples were collected for 4 storms, 3 during known seeding events and one during a nonseeding event (Figure 4). There is a replicated cloud seeding signature for all 3 seeding events. Interestingly, the Ag seeding signature concentration varies over the storm profile, even when seeding occurs over the duration of the storm. This is best illustrated in the data for the post-cold frontal system on Feb 18, 2016. Precipitation

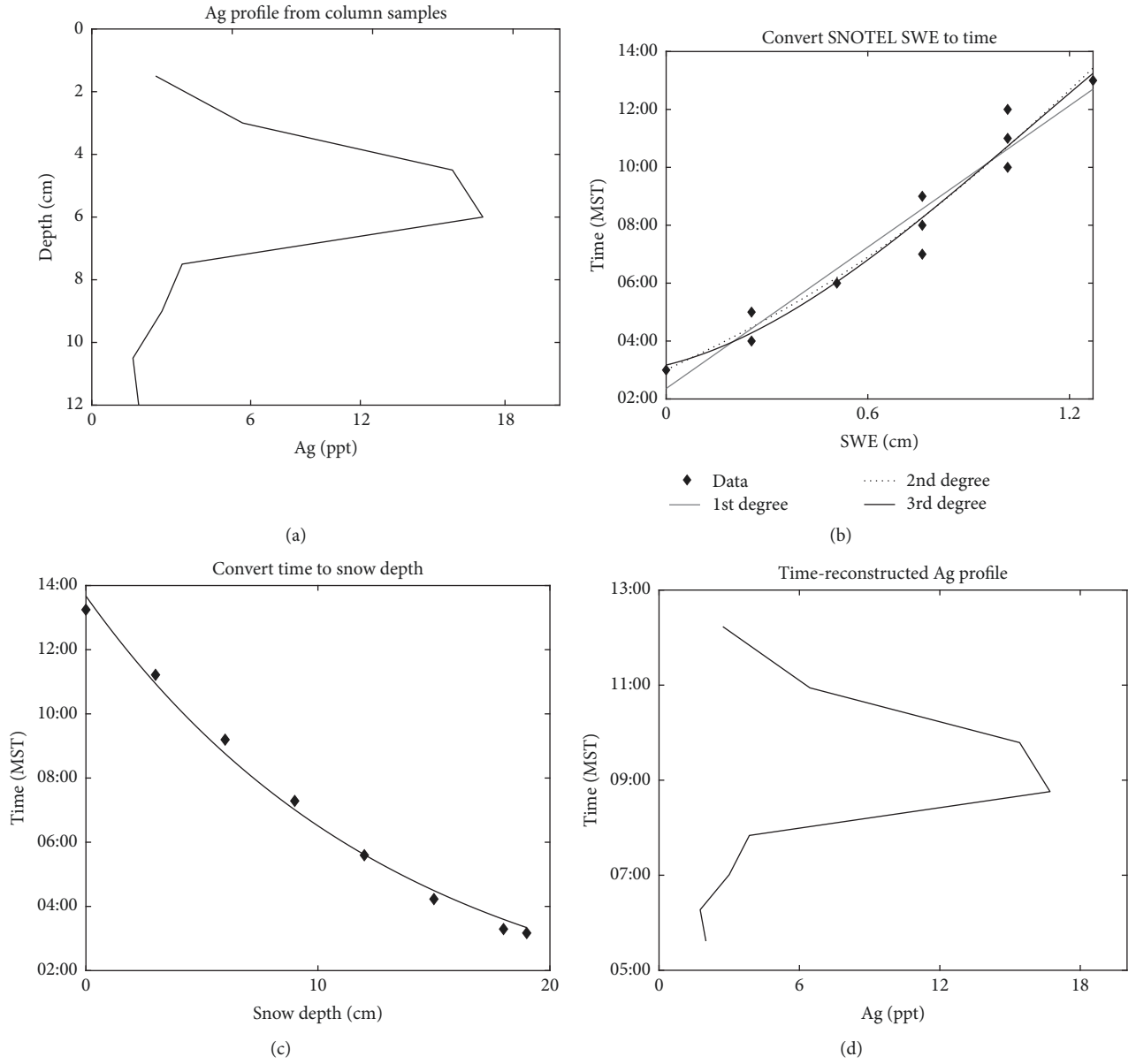

Figure 2: (a) Typical column sample profile, collected at 1.5 cm resolution. (b) Time and SWE from a SNOTEL station nearest to the snow pit collected in plot (a). 1st-, 2nd-, and 3rd-degree polynomials model these relationships. (c) Depth in the snow pit related to time from plot (b). (d) Time-reconstructed Ag profile.

Table 3: Observed seeding signatures for ground and areal-based events.

Snow pits sampled in the target zone	G	A	A + G
Seeded snow pits sampled	17	0	7
Seeded snow pits with seeding signature	15	8	7
% seeded snow pits with an Ag enrichment	88%	0%	100%

developed in a multilayered storm with west southwesterly flow following the frontal passage. Seeding was ongoing from 17:43 to 21:39 MST but a distinct peak in Ag concentration is only observed at 19:45 MST. Overall, ground generator seeding events usually produced seeding signatures for 20–75% of the duration of cloud seeding (Table 4).

The empirical model that uses nearby SNOTEL data to convert depth data of a snow pit sample to time (Section 3.3) effectively constrains the timing of AgI seeded snow deposition (Figure 2), suggesting this approach can provide an alternative to more labor-intensive real-time sampling. Temporal errors, when compared to observed real-time data,

Table 4: Summary of sampling events (excluding snow collected for method development and downwind campaigns).

Storm date	Number of sites sampled	Seeding method[1]	Sites sampled	Samples with seeding signal[2]	Peak Ag [ppt]	Aircraft AgI released [kg]	Generator AgI released [kg]	Wind speed [m s^{-1}][3]	Wind direction[3]	Min/max temperature [C][3]
Mar 24, 2015	6	Ground	3, 4, 5, 6, 7, 8	44%	21	<0.05	1.4	3.4	W	−3.9/0.6
Apr 5, 2015	2	Ground	3, 6	47%	19	-	1.5	1.3	W	−2.2/1.1
Nov 19, 2015	3	Air & ground	3, 3, 5	0%	2.8	2.1	<0.05	1.3	W	−6.1/−0.6
Dec 4, 2015	3	Ground	3, 5, 6	62%	37	-	2.1	3.8	W	−1.1/0.0
Dec 7, 2015	1	Air & ground	6	20%	14	0.2	0.8	4.2	W	0.0/1.1
Dec 9, 2015	1	Air	6	0%	3.0	0.5	-	4.0	W	0.0/2.2
Dec 10, 2015	1	Air	6	0%	1.7	0.2	-	5.8	SW	−1.1/0.6
Dec 13, 2015	1	Air & ground	5	13%	3.1	2.6	2.4	5.8	S	−2.2/0.0
Dec 19-20, 2015	3	Ground	3, 6, 8	75%	9.5	-	1.2	3.3	SW	−6.7/−5.6
Dec 21, 2015	3	Air & ground	3, 6, 8	73%	80	0.9	5.6	4.9	SW	−6.1/0.0
Jan 28-29, 2016	3	Air	3, 5, 8	0%	2.6	2.0	-	5.1	SW	−3.3/1.1
Feb 18, 2016	4	Ground	2, 3, 5, 10	58%	14	-	1.3	5.0	SW	−2.2/−1.1
Apr 14, 2016	1	Air & ground	6	93%	7.3	1.4	0.4	1.3	SW	−1.1/1.1

[1] A: aircraft; G: ground generator. [2] "Seeding signal" is defined as replicated Ag concentrations greater than 3 ppt and a CEF exceeding 2; [3] ground-level data from NWS station KNST, roughly 15 km east of the Payette River Basin border.

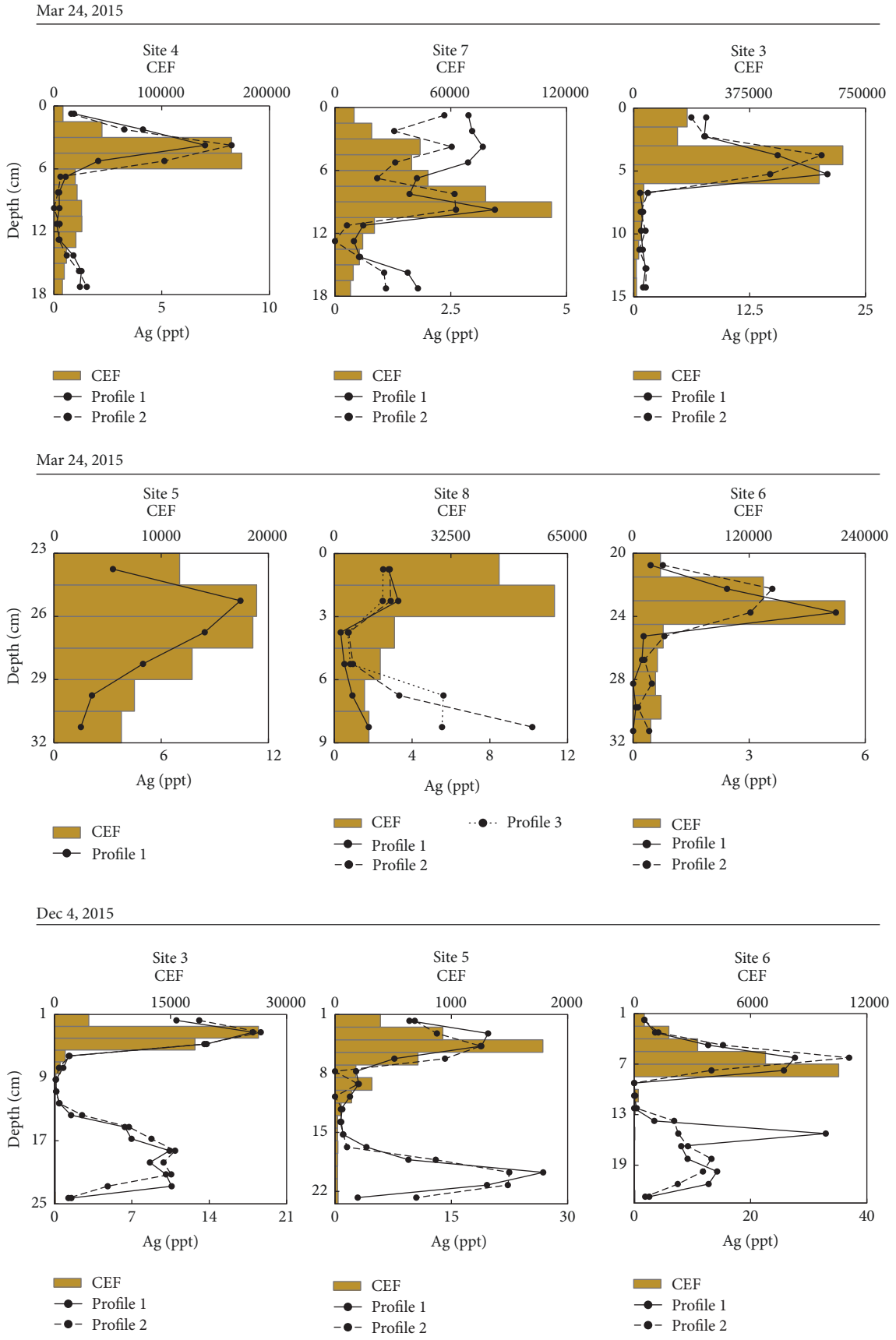

Figure 3: Continued.

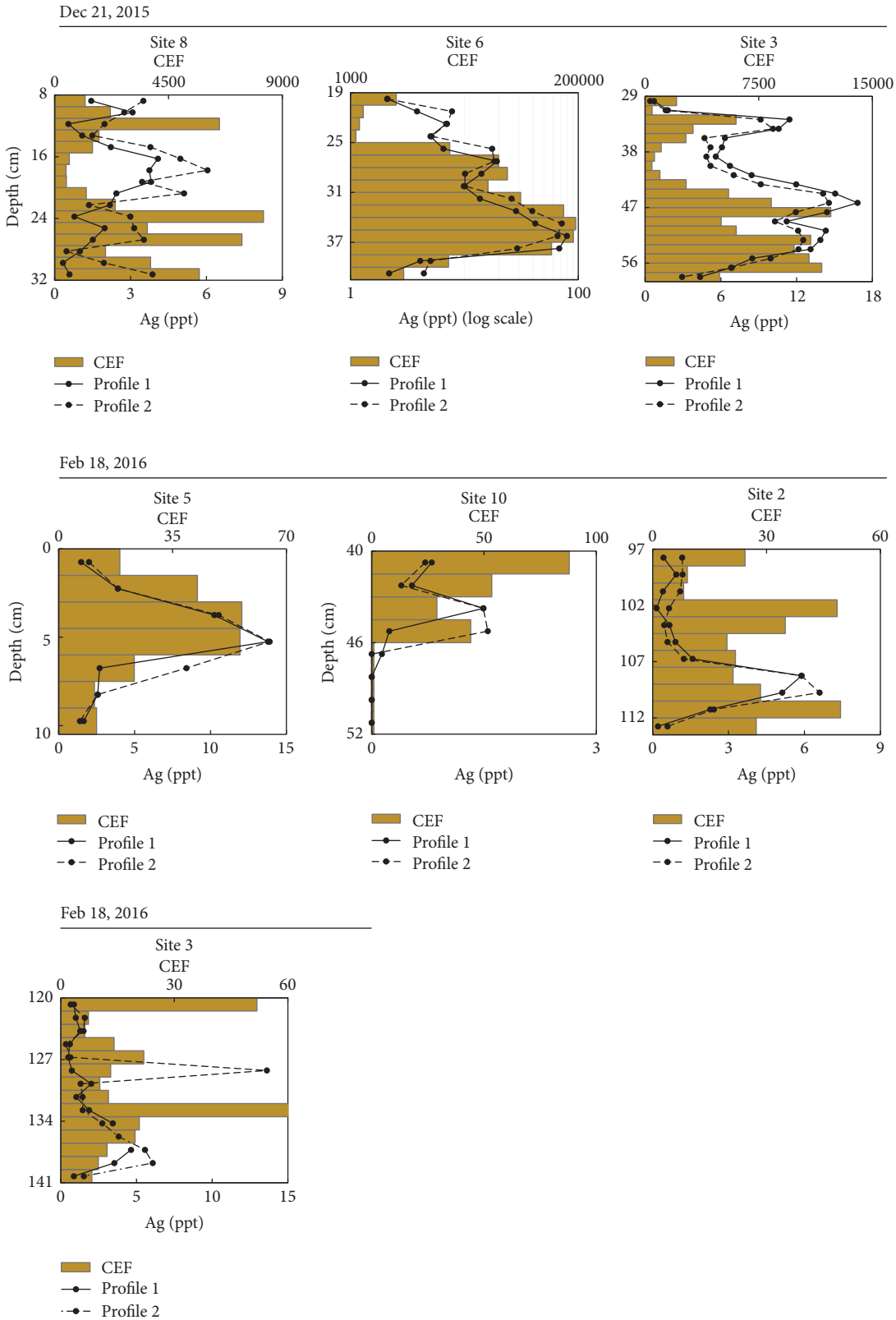

Figure 3: Results for the four spatial sampling campaigns mentioned within the target zone with at least one Ag enrichment are pictured. Solid and dotted black lines are two profiles of samples collected using the column method. Gold horizontal bars denote the enrichment factor with each sample.

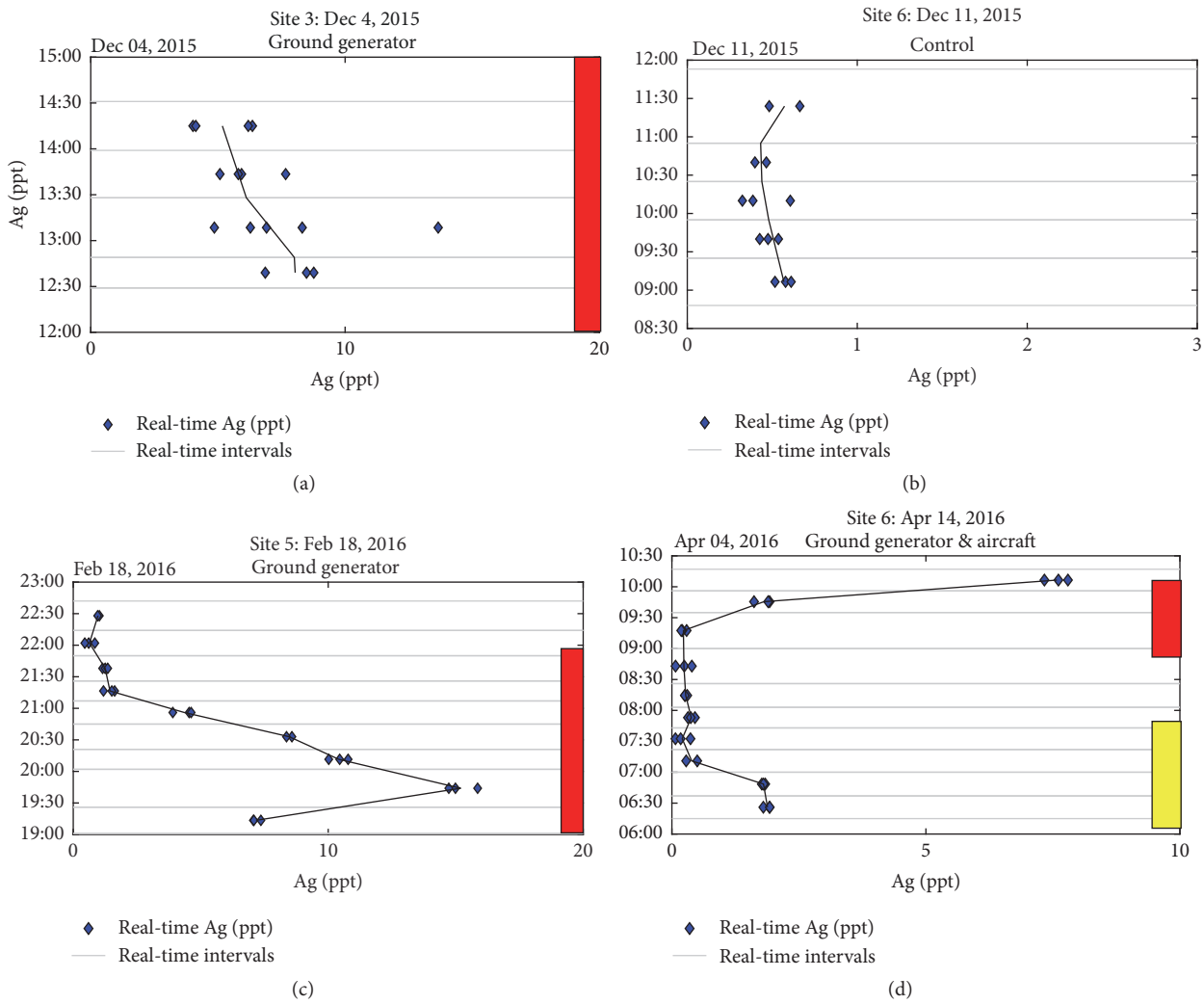

Figure 4: All 4 real-time sampling results from the season. Red bars denote times of ground generator seeding. Yellow bars denote aircraft seeding. Light grey lines delineate sampling intervals. Blue diamonds denote silver concentrations of samples collected during the time delineated between the grey lines.

are less than one hour (Figure 5). When this approach is applied to multiple sites extending down wind, it is possible to track the Ag enrichments through time and space (Figure 6). The plume in Figure 6 is calculated using linear regression of all starting and ending points of modeled Ag enrichment times. Ag enrichments are constrained from 03:58 to 07:40 MST 4.8 km downwind of ground generators but 09:23 to 14:03 MST 38.5 km downwind of ground generators. This suggests that the head of the plume would be moving only 1.8 m s^{-1} while surface winds averaged 3.4 m s^{-1} during the seeding event.

4.4. Downwind Seeding Effects. There is evidence of a consistent Ag seeding signature within 60 km downwind of a ground generator, but the fidelity of those signals beyond this distance is degraded. This is best illustrated by December 21, 2015, storm in Figure 3. This storm system had a tap of Pacific moisture being advected into the target area from southern Oregon producing a prolonged column of deep saturated air over the target area. Samples collected at site 5 (60 km downwind) are enriched at the same times as sites 2 and 3, but with a fraction of the maximum replicated Ag concentration (4 ppt relative to 18 ppt and 80 ppt, resp.). Ag concentrations at site 5 are always within 2 ppt of the minimum threshold defined for seeding signatures. Therefore, 60 km represents the greatest downwind distance of a definitive signal. Some samples (also from the Dec 21, 2015 storm) indicate a possible cloud seeding signature (enrichment factor of 2100, Ag concentration of 4.5 ppt) approximately 80 km downwind. These data indicate that silver enrichments within the target zone are widespread and replicable (Figure 3).

The sampling campaign 180 km downwind of ground generators lacks definitive evidence for AgI nucleation. The nine-site sampling transect is along the Lost River Range, Idaho. Of the 678 total samples in this transect, only 9 samples (~1%) exceed 5 ppt. Of those 9 samples, 8 are located in

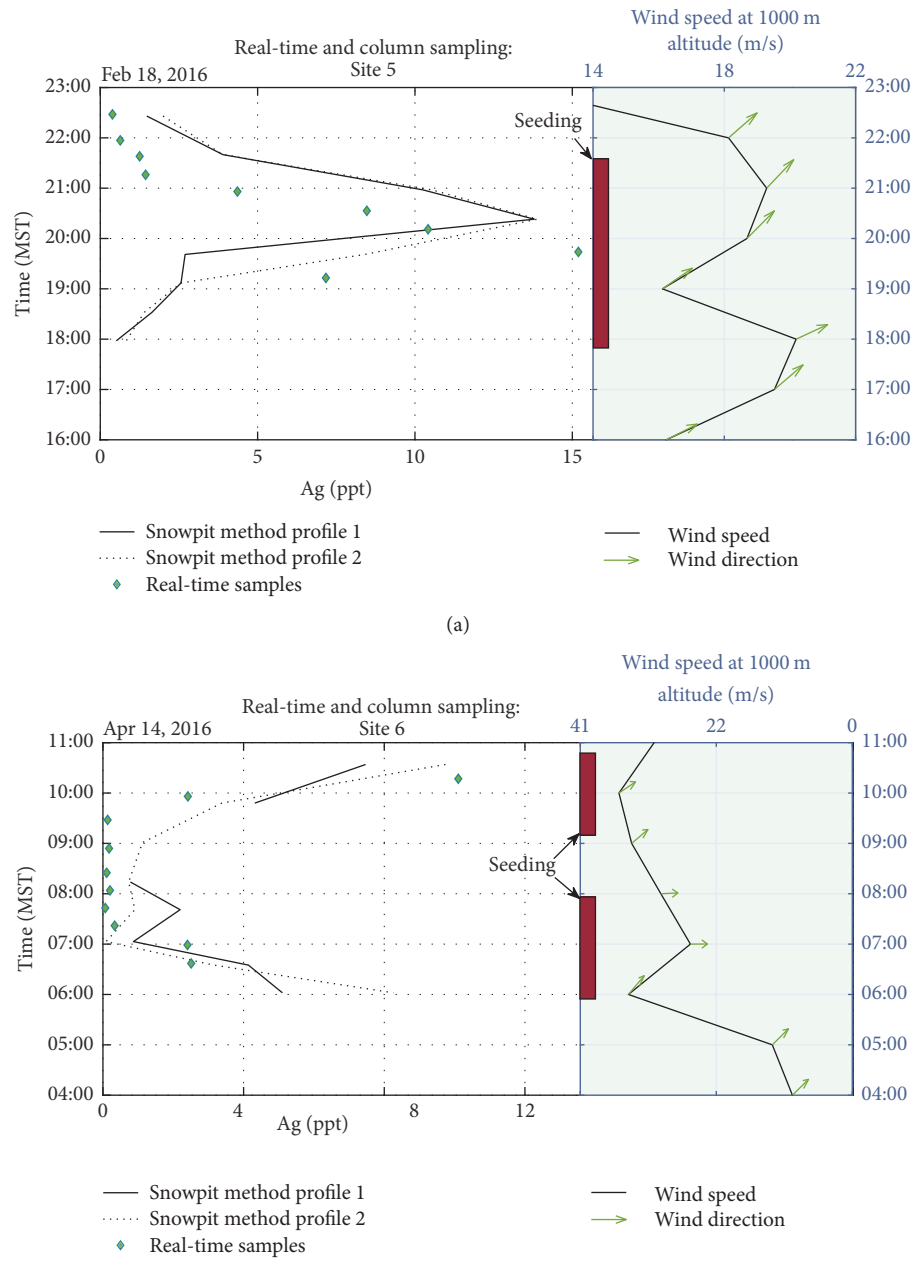

FIGURE 5: Validation of time-delineation methods. We compare real-time samples (green diamonds) with time-delineated column samples (each black line is a profile of column samples). Wind speed and direction are plotted to the right with red bars delineating times of active seeding. Of the 17 ground generators, 16 and 17 were active for sites 5 and 6, respectively.

the southern Lost River Range and were deposited during the February 18 ground generator seeded storm event. The other three storm events combined do not contain a sample containing 5 ppt Ag and an CEF of at least 2.

5. Discussion

5.1. Strong Ag Seeding Signal Observations. It is highly likely that the observed elevated silver concentrations reflect a seeding signature. It is possible that silver sources could come from anthropogenic contamination during sampling or analysis, terrestrial contamination, and/or scavenging of AgI. However, the probability of these silver enrichments from alternative sources is unlikely for several reasons. First, a minimum of two field replicates and three lab replicates are analyzed for each site; these samples do not exhibit evidence of anthropogenic contamination. Second, enrichment factors are employed to account for potential terrestrial contamination. Third, AgI has an extraordinarily low scavenging efficiency [5, 6, 42], so relatively high concentrations of

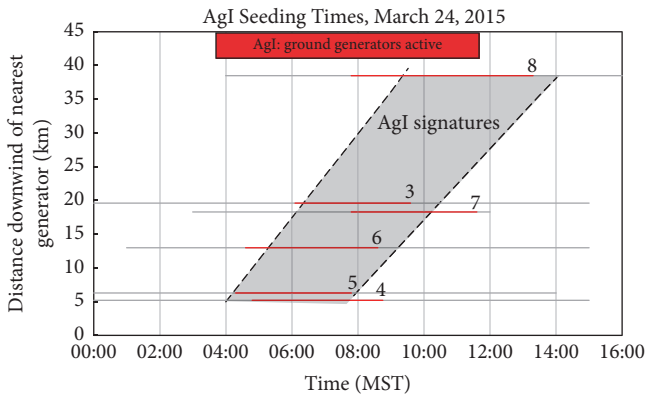

Figure 6: The time-delineation methods constrained the timing of Ag enrichments in snow for the Mar 24, 2015, storm (ground generator only). Red lines denote modeled times with replicated AgI signals. Grey lines denote portions of the snowstorm void of seeding signatures. Black numbers on plot are site IDs corresponding to Figure 1.

silver (>3 ppt) in snow are unlikely to result from scavenging alone. Therefore, it is likely that AgI plumes are delivered to the targeted clouds at concentrations and times to promote nucleation activity.

5.2. Spatial Distribution of AgI. A key outcome of this study is that replicated seeding signatures are present in snow for 88% of ground generator seeding events. Samples from ground generator seeding events also contain relatively higher silver concentrations compared to those collected during aircraft events, often exceeding 15 ppt. Aircraft-only seeding events, on the other hand, do not contain a replicated seeding signature exceeding 10 ppt. Warburton's (1971) study in the Tahoe Truckee Basin also found aircraft signals difficult to detect despite strong signals from ground generators [16].

There are at least four potential reasons aircraft seeding are not consistently detected with trace chemistry. First, aircraft seeding events tended to release less total mass of silver than ground generators in the storms sampled (Table 4). The amount of silver released during aircraft seeding events may have been too low to detect in snow above natural background concentrations. Second, aircraft seeding signatures may be missed by sampling point locations because these signals are not released continuously from a fixed point like ground generators. IPC aircraft flight patterns tend to navigate perpendicular to the mean wind direction during seeding, so it is possible that sampling locations were simply missed by these AgI plumes. Third, AgI may nucleate snow that falls outside the sampled area. Fourth, the efficacy of aircraft seeding may be more sensitive to antecedent drop size and ice nucleus concentrations than ground generators [43], so it is also possible that aerosol concentrations prior to seeding (from dust or pollution) preferentially impeded efficient aircraft seeding.

Spatial sampling results suggest that trace chemistry detection of Ag may be of limited value for assessing aircraft-based cloud seeding efforts. In contrast, Ag enrichments from ground-generated seeding are often detectable and, therefore, tracking Ag in the deposited snow appears to be an effective tool for quantifying this form of cloud seeding. Ground generator targeting was observed to be as great as 60 km downwind of AgI sources. Our data also confirm that seeding signatures are replicable within the basin [20] and silver enrichments are present at all sampled sites in the target zone following a seeding event.

5.3. Temporally Constraining AgI. This study shows that real-time sampling is an effective method at revealing not only if, but also when, seeded snow is deposited. The effectiveness of this method was demonstrated by, for the first time, performing field-validation tests. Two previous studies performed real-time sampling [5, 14] but both of these studies lacked the field replication or method validation testing to corroborate results. This study provides 3 field replicates for each time interval while demonstrating a high degree of replicability. The project standard deviation for each time interval was 0.41 ppt Ag, only 0.02 ppt above our laboratory limit of detection. The results from these real-time samples further validate expected results from ground-based cloud seeding and represent highly constrained data, both in space and in time, for model validation.

Real-time snow collection agrees with activation times of upwind ground generators. Silver enrichments were observed at all three sampled seeded events. Two events appear to capture the head or tail of the AgI plume. Real-time samples identify silver enrichments within 30 minutes of the plume entering or leaving the region. The 30-minute lag of signals to AgI release approximately corresponds with estimated travel times from the AgI source to the real-time sampling site. Conversely, real-time samples that were collected during a natural storm event (unseeded) contained silver concentrations less than 1 ppt for all 15 samples. This agrees with background silver concentrations previously measured for Payette Basin snow [36, 38].

Interestingly, seeding signatures in snow are often observed in short-lived pulses, even when seeding was conducted throughout the event. This observation is not consistent with the continuous flux of Ag from the ground generators producing similar Ag concentrations for the duration of seeding. This pulse-like trend is best illustrated by the Feb 18, 2016, real-time data (Figure 4), but also evident in most pit sample profiles (Figure 3). There are several potential explanations for this trend. First, it is possible that shifting winds produce a wandering track of seeded snow deposition that is only observed at a given location when the track produces snow accumulation at that point. A second interpretation is that cloud seeding enhancement occurs over the entire time period but the pulses of Ag seeding signature represent a relative shift between direct nucleation (high Ag concentrations) and secondary ice formation processes originally stimulated by AgI (low Ag concentrations). In any case, the collection of a larger, spatially distributed, real-time dataset would help explain these observations and provide additional insight into cloud seeding performance. Based on these observations, direct AgI nucleation may be limited

to a fraction of the period during which active seeding is occurring.

5.4. Downwind Seeding Effects. Two recent literature reviews cumulatively list more than 26 studies implying AgI seeding increases precipitation beyond 70 km [44, 45], suggesting the potential for seeding signatures. However, this study shows that the maximum spatial extent of seeding signatures from ground generators is approximately 60 km downwind of AgI sources. This observation is similar to the findings of the only other known downwind trace chemical study [16]. Warburton (1971) also found background Ag concentrations in snow at downwind sites. However, these results were obtained prior to known clean methods and should be interpreted cautiously.

A variety of factors may explain the lack of physical evidence for AgI seeding beyond 70 km. First, photolytic deactivation renders AgI ineffective after a prolonged exposure to direct light. Prior studies estimate that photolytic deactivation occurs about 90 minutes [17, 46] after release. Assuming 45 km h^{-1} winds at the supercooled liquid water level and seeding took place during daylight hours, detectable signatures will begin to diminish about 70 km downwind. Second, the deposition of AgI in the target zone, fused with the dispersion of the remaining AgI downwind, will likely dilute the available aerosols downwind [47]. This could reduce the AgI signal to near background levels, even when enhanced snow deposition has occurred. Lastly, sampling snow for seeding Ag signatures more than 48 hours after a storm poses several challenges. Compaction of the snow results in a potential dilution of seeding signature. If the thickness of snow sampled using the snow pit method exceeds the thickness of seeded snow, then compaction dilutes the signal. In summary, there is limited evidence of seeding effects beyond about 70 km downwind. It is possible that the source-receptor approach is not an effective method at detecting cloud seeding evidence at these distances.

6. Conclusions

Spatial sampling results demonstrate the widespread and replicable observation of Ag seeding signatures in the snowpack within the area targeted for enhancement. In almost all instances, silver enrichments are identified and replicated for all sites seeded by ground generators. Sampling of aircraft seeding events, conversely, does not reveal physical evidence in snowpack. Only 11% of airborne-seeded sampling sites contain a replicated seeding signature. The reason for this dichotomous observation is not clear, but it is potentially due to aircraft seeding releasing less AgI that produces concentrations not detectable above natural background.

A validated field method was developed for collecting real-time samples of snow suitable for trace element analysis. This real-time sampling method produces replicable results and provides useful data to constrain timing of AgI deposition. Real-time sampling, along with time-reconstructed column sampling, constrains AgI signals within the nearest hour and is a promising tool for evaluating cloud seeding operations.

The maximum downwind extent of an observed Ag seeding signature is at least 60 km with limited evidence suggesting seeding signatures up to about 70 km. The lack of Ag observations beyond 70 km may be attributed to the lower concentrations of AgI downwind due to dispersion and upwind nucleation.

Conflicts of Interest

The authors wish to declare that James Fisher, Mel Kunkel, Shaun Parkinson, Derek Blestrud, and Nick Dawson are currently employed by the Idaho Power Company. Ross Edwards was previously a consultant for Idaho Power's cloud seeding program. Shawn Benner and Marion Lytle are employed by Boise State University.

Acknowledgments

The authors would like to thank Matt Masarik, Katelyn Watson, Miguel Aguayo, and Reggie Walters for their assistance in data analysis. They appreciate Mark Schmitz for giving them access to his facilities and for technical help with laboratory analysis. They would also like to thank Rob Florence, Andy Karlson, Clay Roehner, Kerrie Weppner, and Larry Thomas Oltheim ("TomO") for their assistance in sample collection. Finally, they would like to acknowledge Heritage Environmental Consultants in Golden, CO, for funding this work.

References

[1] The National Research Council, *Critical Issues in Weather Modification Research*, The National Academies Press, Washington, D.C, USA, 2003.

[2] D. Reynolds, "Literature review and scientific synthesis on the efficacy of winter orographic cloud seeding , CIRES, Boulder, CO," *A report to the U.S. Bureau of Reclamation*, 2015.

[3] M. J. Manton, L. Warren, S. L. Kenyon, A. D. Peace, S. P. Bilish, and K. Kemsley, "A confirmatory snowfall enhancement project in the snowy mountains of Australia. Part I: Project design and response variables," *Journal of Applied Meteorology and Climatology*, vol. 50, no. 7, pp. 1432–1447, 2011.

[4] B. Pokharel, B. Geerts, and X. Jing, "The impact of ground-based glaciogenic seeding on clouds and precipitation over mountains: A case study of a shallow orographic cloud with large supercooled droplets," *Journal of Geophysical Research: Atmospheres*, vol. 120, no. 12, pp. 6056–6079, 2015.

[5] J. A. Warburton, R. H. Stone III, and B. L. Marler, "How the transport and dispersion of AgI aerosols may affect detectability of seeding effects by statistical methods," *Journal of Applied Meteorology and Climatology*, vol. 34, no. 9, pp. 1929–1941, 1995.

[6] S. K. Chai, W. G. Finnegan, and R. L. Pitter, "An interpretation of the mechanisms of ice-crystal formation operative in the Lake Almanor cloud-seeding program," *Journal of Applied Meteorology and Climatology*, vol. 32, no. 11, pp. 1726–1732, 1993.

[7] J. A. Warburton, L. G. Young, and R. H. Stone, "Assessment of seeding effects in snowpack augmentation programs: ice nucleation and scavenging of seeding aerosols," *Journal of Applied Meteorology and Climatology*, vol. 34, no. 1, pp. 121–130, 1995.

[8] L. Xue, X. Chu, R. Rasmussen, D. Breed, B. Boe, and B. Geerts, "The dispersion of silver iodide particles from ground-based generators over complex terrain. Part II: WRF large-eddy simulations versus observations," *Journal of Applied Meteorology and Climatology*, vol. 53, no. 6, pp. 1342–1361, 2014.

[9] L. Xue, R. Edwards, A. Huggins et al., "WRF Large-eddy Simulations of chemical tracer deposition and seeding effect over complex terrain from ground- and aircraft-based AgI generators," *Atmospheric Research*, vol. 190, pp. 89–103, 2017.

[10] L. Xue, S. A. Tessendorf, E. Nelson et al., "Implementation of a silver iodide cloud-seeding parameterization in WRF. Part II: 3D simulations of actual seeding events and sensitivity tests," *Journal of Applied Meteorology and Climatology*, vol. 52, no. 6, pp. 1458–1476, 2013.

[11] J. French and B. Geerts, "SNOWIE: Seeded and Natural Orographic Wintertime clouds: the Idaho Experiment," *National Science Foundation reward*, Article ID 1547101, 2016.

[12] WWMPP., "The Wyoming Weather Modification Pilot Project: Level II study. Executive draft summary," http://wwdc.state.wy.us/weathermod/WYWeatherModPilotProgramExecSummary.pdf, 2014.

[13] A. Huggins, "Summary of studies that document the effectiveness of cloud seeding for snowfall augmentation," *J. Weather Modif*, vol. 41, pp. 127–134, 2009.

[14] A. Huggins, *Trace Chemical Monitoring for the Wyoming Weather Modification Pilot Project: Tasks for the 2010 Field Project*, Desert Research Institute, 2010.

[15] A. Huggins, S. Kenyon, L. Warren, A. Peace, S. Billish, and M. Manton, "The Snowy Precipitation Enhancement Research Project: A Description and Preliminary Results," *J. Weather Modif*, vol. 40, pp. 28–53, 2008.

[16] J. Warburton, "Physical evidence of transport of cloud-seeding materials into areas outside primary targets," in *Proceedings of International Conference on Weather Modification*, pp. 185–190, Canberra, Australia, 1971.

[17] A. B. Super, J. T. McPartland, and J. A. Heimbach, "Field observations of the persistence of AgI-NH," *Journal of Applied Meteorology and Climatology*, vol. 14, no. 8, pp. 1572–1577, 1975.

[18] A. Huggins, R. Edwards, and J. McConnell, "Summary of trace chemical and physical measurements of snowfall in two Nevada cloud seeding target areas," in *Desert Res. Inst*, pp. 1–5, Reno NV, 2005.

[19] M. Johannessen and A. Henriksen, "Chemistry of snow meltwater: Changes in concentration during melting," *Water Resources Research*, vol. 14, no. 4, pp. 615–619, 1978.

[20] J. Fisher, M. Lytle, M. Kunkel et al., "Trace chemical evaluation of cloud seeding in the Payette Basin," *J. Weather Modif*, vol. 48, pp. 24–42, 2016.

[21] E. Snyder-Conn, J. R. Garbarino, G. L. Hoffman, and A. Oelkers, "Soluble trace elements and total mercury in arctic alaskan snow," *Arctic*, vol. 50, no. 3, pp. 201–215, 1997.

[22] J. I. López-Moreno, S. R. Fassnacht, S. Beguería, and J. B. P. Latron, "Variability of snow depth at the plot scale: Implications for mean depth estimation and sampling strategies," *The Cryosphere*, vol. 5, no. 3, pp. 617–629, 2011.

[23] M. C. Serreze, M. P. Clark, R. L. Armstrong, D. A. McGinnis, and R. S. Pulwarty, "Characteristics of the western United States snowpack from snowpack telemetry (SNOTEL) data," *Water Resources Research*, vol. 35, no. 7, pp. 2145–2160, 1999.

[24] N. P. Molotch and R. C. Bales, "Scaling snow observations from the point to the grid element: Implications for observation network design," *Water Resources Research*, vol. 41, no. 11, Article ID W11421, pp. 1–16, 2005.

[25] N. Dawson, P. Broxton, X. Zeng, M. Leuthold, M. Barlage, and P. Holbrook, "An evaluation of snow initializations in NCEP global and regional forecasting models," *Journal of Hydrometeorology*, vol. 17, no. 6, pp. 1885–1901, 2016.

[26] B. McGurty, "Turning silver into gold: Measuring the benefits of cloud seeding," *Hydro Rev*, vol. 18, no. 1, pp. 2–6, 1999.

[27] A. B. Super and B. A. Boe, "Microphysical Effects of Wintertime Cloud Seeding with Silver Iodide over the Rocky Mountains. Part III: Observations over the Grand Mesa, Colorado," *Journal of Applied Meteorology and Climatology*, vol. 27, no. 10, pp. 1166–1182, 1988.

[28] R. Woodriff, B. R. Culver, D. Shrader, and A. B. Super, "Determination of sub-nanogram quantities of silver in snow by furnace atomic absorption spectrometry," *Analytical Chemistry*, vol. 45, no. 2, pp. 230–234, 1973.

[29] C. Boutron, "Reduction of contamination problems in sampling of antarctic snows for trace element analysis," *Analytica Chimica Acta*, vol. 106, no. 1, pp. 127–130, 1979.

[30] C. F. Boutron, "A clean laboratory for ultralow concentration heavy metal analysis," *Fresenius' Journal of Analytical Chemistry*, vol. 337, no. 5, pp. 482–491, 1990.

[31] I. Rodushkin, E. Engström, and D. C. Baxter, "Sources of contamination and remedial strategies in the multi-elemental trace analysis laboratory," *Analytical and Bioanalytical Chemistry*, vol. 396, no. 1, pp. 365–377, 2010.

[32] W. Telliard, *Method 200.8: Determination of Trace Elements in Waters and Wastes by Inductively Coupled Plasma - Mass Spectrometry*, Environmental Protection Agency, Revision 5.5 EMMC Version, 2008.

[33] B. G. Koffman, M. J. Handley, E. C. Osterberg, M. L. Wells, and K. J. Kreutz, "Dependence of ice-core relative trace-element concentration on acidification," *Journal of Glaciology*, vol. 60, no. 219, pp. 103–112, 2014.

[34] L.-S. Wen, P. H. Santschi, G. A. Gill, and D. Tang, "Silver concentrations in Colorado, USA, watersheds using improved methodology," *Environmental Toxicology and Chemistry*, vol. 21, no. 10, pp. 2040–2051, 2002.

[35] T. W. Purcell and J. J. Peters, "Sources of silver in the environment," *Environmental Toxicology and Chemistry*, vol. 17, no. 4, pp. 539–546, 1998.

[36] R. Edwards, A. Huggins, and J. McConnell, *Trace chemistry evaluation of the IPCo 2003-3004 cloud seeding program*, Desert Research Institute, 2004.

[37] S. R. Taylor and S. M. McLennan, "The chemical composition evolution of the continental crust," *Reviews of Geophysics*, vol. 33, no. 2, pp. 241–265, 1995.

[38] Cardno ENTRIX, "Geochemistry and Impacts of Silver Iodide Use in Cloud Seeding.", Available: http://www.weathermodification.org/enviro&techdocs/Entrixreport.pdf, 2011

[39] J. Fisher, S. Benner, M. Lytle, P. Golden, and R. Edwards, *Trace chemical evaluation of cloud seeding in the payette basin, heritage environmental consultants*, CO, Golden, 2016.

[40] P. V. Hobbs, "The nature of winter clouds and precipitation in the cascade mountains and their modification by artificial seeding. part I: natural conditions," *Journal of Applied Meteorology and Climatology*, vol. 14, no. 5, pp. 783–804, 1975.

[41] P. V. Hobbs, "The nature of winter clouds and precipitation in the cascade mountains and their modification by artificial seeding. part III: case studies of the effects of seeding," *Journal of*

Applied Meteorology and Climatology, vol. 14, no. 5, pp. 819–858, 1975.

[42] A. Dennis, *Weather Modification by Cloud Seeding*, vol. 24, Academic Press, New York, NY, USA, 1980.

[43] D. W. Reynolds, "A report on winter snowpack-augmentation," *Bulletin of the American Meteorological Society*, vol. 69, no. 11, pp. 1435–1456, 1988.

[44] S. Hunter, "Comprehensive literature survey on the potential extra-area precipitation effects of winter cloud seeding," Denver, CO, Final Report submitted to the Colorado Water Conservation Board, 2009.

[45] T. P. DeFelice, J. Golden, D. Griffith et al., "Extra area effects of cloud seeding - an updated assessment," *Atmospheric Research*, vol. 135-136, pp. 193–203, 2014.

[46] T. Deshler and D. W. Reynolds, "The persistence of seeding effects in a winter orographic cloud seeded with silver iodide burned in acetone," *Journal of Applied Meteorology and Climatology*, vol. 29, no. 6, pp. 477–488, 1990.

[47] U. S. Senate, "Weather Modification: Programs, Problems, Policy, And Potential," in *Committee on Commerce - Science and Transportation*, pp. 1–645, Washington, D.C, USA, 1978.